

## Synthesis and Thermal Properties of Cellulose-based Polycaprolactones

Hyoe Hatakeyama\*, Takanori Yoshida, Yoshinobu Izuta

Fukui University of Technology, 3-6-1 Gakuen, Fukui, Fukui 910-8505, Japan

Shigeo Hirose

National Institute of Materials and Chemical Research, Tsukuba, Ibaraki 305-8565, Japan

Tatsuko Hatakeyama

Otsu Women's University, 12 Sanbancho, Chiyodaku, Tokyo 102-8357, Japan

**SUMMARY:** Cellulose-based polycaprolactone (CAPCL) sheets were prepared from cellulose acetate (CA) and  $\epsilon$ -caprolactone (CL). Thermal properties of the obtained CAPCL's were studied by differential scanning calorimetry (DSC), thermogravimetry (TG) and TG-Fourier transform infrared spectrometry (TG-FTIR). The glass transition temperatures ( $T_g$ 's) of CAPCL decreased with increasing CL/OH ratio, until CL/OH ratio reached 15 and then increased above that ratio. Melting of CAPCL was observed when CL/OH ratio was over 10. The thermal degradation temperatures ( $T_d$ 's) of CAPCL increased from ca. 350 °C to 390 °C with increasing CL/OH ratio. The results obtained by TG-FTIR analysis of CAPCL showed that gases with OH, CH, C=O, C-O-C groups evolved by thermal degradation.

## Introduction

In the past 15 years, various synthetic polymers, which can be derived from plant components such as saccharides and lignin, have extensively been investigated by various research groups<sup>1-13)</sup>. The polyurethane's (PU's) were prepared from various types of plant components at our laboratory and it was found that their mechanical and thermal properties can be controlled by appropriate molecular design. They were biodegraded by microorganisms when they were placed in soil<sup>9)</sup>. In our recent study<sup>13)</sup>, polycaprolactone (PCL) derivatives were synthesized from saccharides such as glucose, fructose and sucrose. PU sheets were also prepared from the above PCL derivatives by the reaction with diphenylmethane diisocyanate (MDI). It was found that the higher-order structure of PU's derived from PCL derivatives vary according to the difference in the molecular association of PCL chains.

In the present study, CAPCL's were synthesized from cellulose acetate (CA) by the reaction with  $\epsilon$ -caprolactone (CL). In this polymer, free hydroxyl groups were used as reaction sites and cellulose having various length of CL chains was prepared. The obtained polymers were characterized with respect to phase transition, thermal degradation and chemical structures of the gases evolved by the thermal degradation of CAPCL.

## Experimental

### Sample Preparation

CAPCL's were synthesized from cellulose acetate (CA: acetyl content, 39.87 %;  $M_w = 6.32 \times 10^4$ ;  $M_w/M_n = 2.27$ ) by the polymerization of CL which was initiated by the OH group of CA. CL/OH (mol/mol) ratios were changed from 2 to 20 (CL/OH ratio = 2, 5, 8, 10, 15 and 20). The polymerizations were carried out for 12 hr at 150 °C with the presence of a small amount of dibutyltin dilaurate (DBTDL). CAPCL sheets were prepared by heat-pressing the synthesized polymers at 160 - 180 °C at ca. 100 kg/cm<sup>2</sup>.

### Measurements

Differential scanning calorimetry (DSC) was performed using a Seiko DSC 220 at a heating rate of 10 °C / min under a nitrogen flow. Sample mass was ca. 5mg. Aluminum open pans were used. The samples were heated to 120 °C and quenched to -150 °C. DSC heating curves of quenched samples were used for analysis. The melting temperature ( $T_m$ ), melting enthalpy ( $\Delta H_m$ ), cold crystallization temperature ( $T_{cc}$ ), glass transition temperature ( $T_g$ ) and heat capacity gap ( $\Delta C_p$ ) were determined by the method reported previously<sup>14</sup>.

Thermogravimetry (TG) was carried out in nitrogen using a Seiko TG 220 at a heating rate of 10 °C / min in the temperature range from 20 to 800 °C. Sample mass was ca. 5mg. TG curves and derivatograms were recorded. Mass loss was indicated as  $[(m_T/m_{20}) / m_{20}] \times 100$  (%) where  $m_T$  is mass at temperature T and  $m_{20}$  is mass at 20°C. Mass residue was evaluated at 450 °C.

Gases evolved by thermal degradation were analyzed by TG-Fourier transform infrared spectrometry (FTIR) using a JASCO FT/IR-420. The heating rate was 20 °C / min in the temperature range from 40 to 800 °C. The flow rate of carrier nitrogen gas was 100 ml/min and the sample weight was 7 to 10 mg. The gas transfer system was maintained at 270 °C. The

resolution power of FTIR was  $4\text{ cm}^{-1}$ . The number of integration was ten and the data incorporation time was 30 s.

## Results and Discussion

### DSC

Figs. 1 and 2 show DSC curves of CAPCL with various CL/OH ratios from 1 to 20. An endothermic peak at around  $50\text{ }^{\circ}\text{C}$  is observed when the CL/OH ratio of the samples exceeds 10, and enthalpy of melting increases with increasing CL/OH ratio. The exothermic peak is clearly observed in the DSC curve of the sample with CL/OH ratio 15. A broad and shallow exothermic deviation can also be observed at a temperature lower than melting for the sample with CL/OH ratio 20. When the DSC heating curves are magnified at a temperature ranging from  $-80$  to  $0\text{ }^{\circ}\text{C}$ , baseline deviation attributed to the glass transition of CAPCL is distinctly observed as shown in Fig. 2. Heat capacity gap at glass transition temperature ( $\Delta C_p$ ) increases with increasing CL/OH ratio. As shown in Fig. 2,  $T_g$  decreases with increasing CL/OH ratio when CL/OH ratio in CAPCL's is below 10 and then increases when CL/OH ratio exceeds 15.

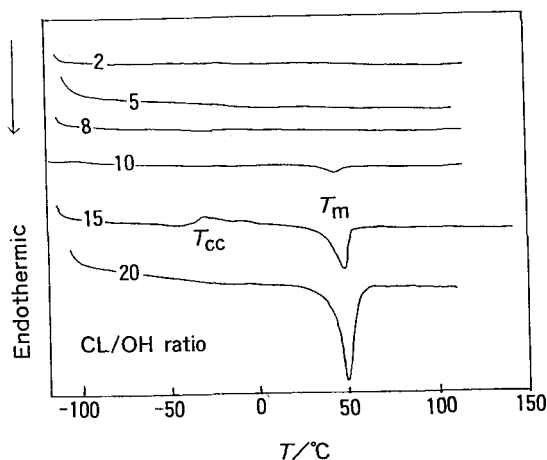


Fig. 1. DSC heating curves of CAPCL  
Numerals in the figure show CL/OH ratio,  $T_m$ ; melting temperature,  
 $T_{cc}$ ; cold crystallization temperature

Fig. 3 shows the relationships between  $T_g$ 's, the heat capacity difference at  $T_g$  ( $\Delta C_p$ ) and CL/OH ratios of CAPCL's. As shown in Fig. 3,  $T_g$  decreases with increasing CL/OH ratio, showing a minimum value when CL/OH ratio is 10, and then increases with increasing CL/OH ratio. In contrast,  $\Delta C_p$  varies in the opposite manner.

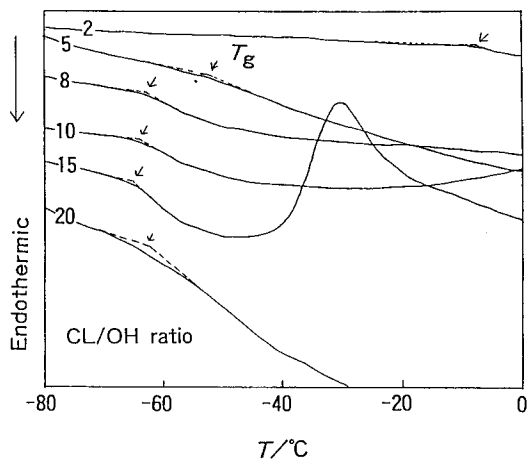


Fig. 2. Magnified DSC heating curves at around  $T_g$  of CAPCL

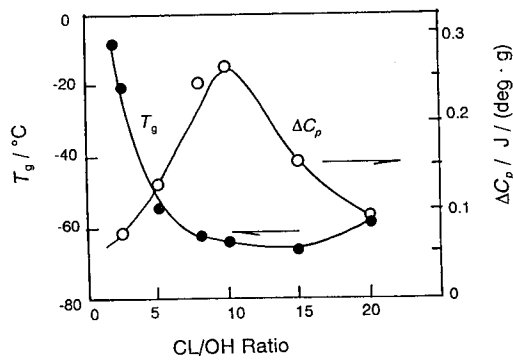


Fig. 3. Relationships between  $T_g$ ,  $\Delta C_p$  and CL/OH ratio in CAPCL

The above results indicate that PCL chains introduced to the glucopyranose ring as side chains act as soft segments in CAPCL. The molecular motion of caprolactone chains is enhanced progressively with increasing chain length of CL chains when CL/OH ratio is below 10. This can be observed as a decrease of  $T_g$  and an increase of  $\Delta C_p$ . However, as shown in Figs. 1 and 2, CL chains form an ordered structure due to coagulation of side chains. This can clearly be seen in the case of the DSC curve of CAPCL with CL/OH ratio of 15, i.e. a prominent exothermic peak due to cold crystallization and a peak of melting of crystals observed at around  $-35$  and  $+50$  °C, respectively. Cold crystallization and melting in the DSC curves suggest that crystalline region is formed in the CAPCL's with CL/OH ratios of 15 and 20. It is reasonable to consider that the molecular motion of random chains is restricted in the presence of ordered structure. A small and shallow exothermic peak and a prominent melting peak observed for the sample with CL/OH ratio 20 indicate that the entirely amorphous sample could not be formed by quenching, but that the crystalline region is rearranged during cooling from  $120$  °C to  $-150$  °C. As shown in Fig. 4,  $T_m$  and  $\Delta H_m$  increase with increasing CL/OH ratio.

The above results suggest that the incorporation of PCL chains into the CA structure leads to the enhancement of molecular motion of CAPCL's. The flexible PCL chains expand inter-molecular distance of CA chains when CL/OH ratio is below 10 and molecular chains become mobile. However, when CL/OH ratio is over 15, CAPCL's with long PCL chains (CL/OH ratio = 15 and 20), the long PCL chains arrange in regular molecular forms and obtained crystalline structure restricts the free molecular motion. As shown in Fig. 3,  $\Delta C_p$  increases in the initial stage and then decreases with increasing CL/OH ratio. This also supports the facts.

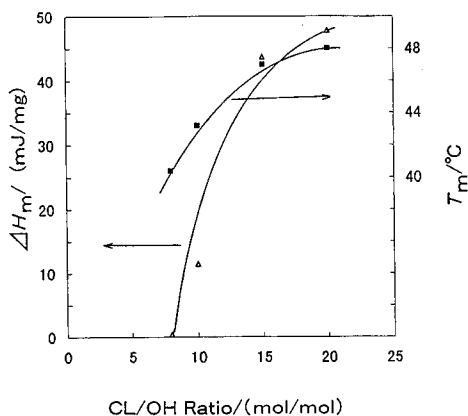


Fig. 4. Relationships between  $T_m$ ,  $\Delta H_m$  and CL/OH ratio in CAPCL

## TG

Fig. 5 shows TG heating curves of CAPCL's with various CL/OH ratios, which were measured in  $N_2$ . In the TG curves of CAPCL's, the start of thermal degradation is recognized at around 350 °C, when CL/OH ratio is 2. As seen from Fig. 5, degradation temperature ( $T_d$ ), which is defined as indicated in the figure, increases with increasing CL/OH ratio. Mass loss of the samples with CL/OH ratio 2 and 5 takes place in one stage, and in contrast mass loss of the samples with CL/OH ratio higher than 8 occurs in multiple stages. TG derivatograms (Fig. 6) show the single peak or multiple peaks corresponding to the TG curves.

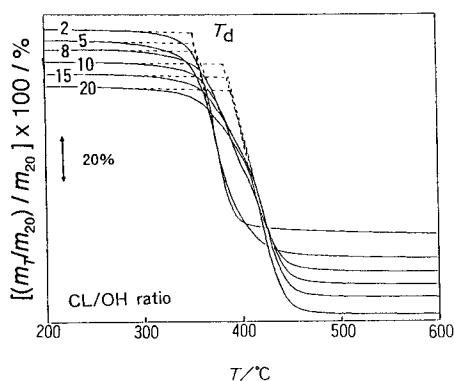


Fig. 5. TG heating curves of CAPCL  
 $m_{20}$ ; mass at 20°C,  $m_t$ ; mass at  $t$   
 Numerals in the figure show CL/OH ratio,  
 $T_d$ ; decomposition temperature

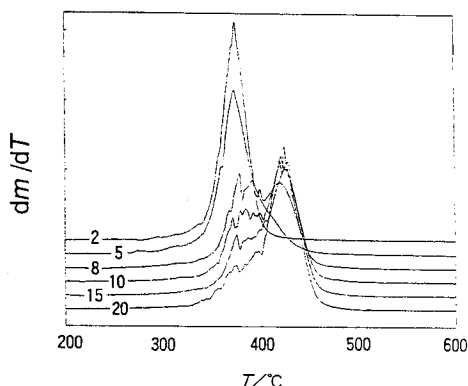


Fig. 6 TG derivatograms

As shown in Fig. 7,  $T_d$ 's of CAPCL increased from ca. 350 °C to 390 °C with increasing CL/OH ratio. From this result, it is considered that the thermal degradation of CAPCL with increased chain length seems to occur with more difficulty, since the ratio of thermally unstable saccharide structure in CAPCL decreased comparatively with increasing amounts of PCL. Fig. 7 also shows the relationship between the mass residue at 450 °C and the CL/OH ratios in CAPCL's. The residue at 450 °C decreases with increasing CL/OH ratio, suggesting that the CA part in CAPCL constitutes a significant part of the residual products. This indicates that the thermal decomposition of PCL chains in CAPCL leads to the production of gaseous products when PCL chains decomposed.

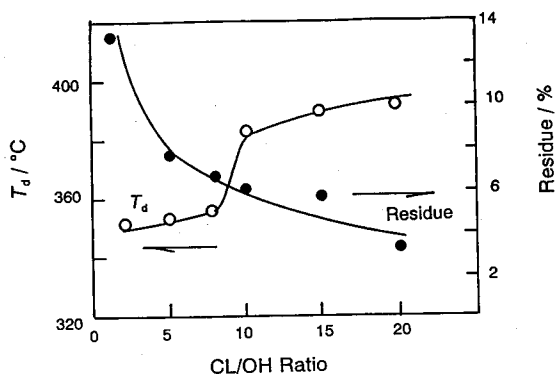


Fig.7. Relationship between  $T_d$ , mass residue and CL/OH ratio in CAPCL

### TG-FTIR

Figs.8 and 9 show the change of TG-FTIR spectra of the CAPCL's with CL / OH ratio = 5 and 15. The IR intensity of the evolved gases from the thermally decomposed CAPCL's increases with increasing CL / OH ratio. The assignments of IR absorption peaks of evolved gases are as follows<sup>15</sup>):  $\text{CO}_2$ , 2358 and 665  $\text{cm}^{-1}$ ;  $\text{NO}_2$ , 1620  $\text{cm}^{-1}$ ;  $\text{C}=\text{C}$ , 1620 and 1510  $\text{cm}^{-1}$ ;  $\text{CH}$ , 2920 and 2850  $\text{cm}^{-1}$ ;  $\text{C-O-C}$ , 1128  $\text{cm}^{-1}$ ;  $\text{C=O}$ , 1720  $\text{cm}^{-1}$ .

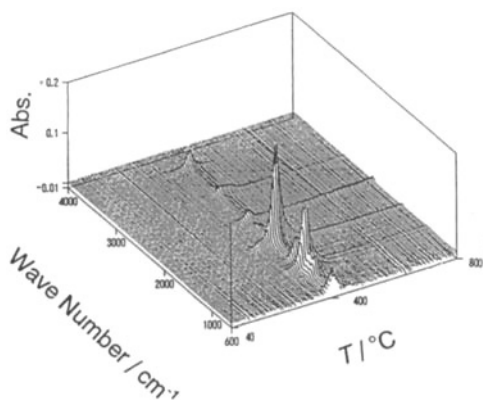


Fig. 8. TG-FTIR of CAPCL (CL/OH ratio = 5 mol/mol)

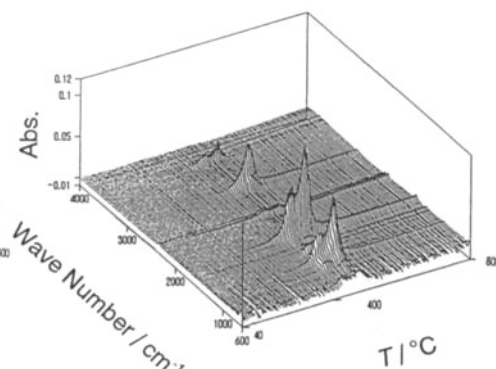


Fig. 9. TG-FTIR of CAPCL (CL/OH ratio = 15 mol/mol)

The results obtained by TG-FTIR analysis of CAPCL showed that  $\text{CO}_2$  and gases with OH, CH, C=O, C-O-C groups were recognizably evolved by the thermal degradation of CAPCL. As shown in Fig. 9, evolved gases with CH structure increase markedly with increasing CL/OH ratio in CAPCL, since the PCL chain consists of  $(-\text{COCH}_2\text{CH}_2\text{CH}_2\text{CH}_2\text{CH}_2-\text{O}-)$  structure. Similarly evolved gases with C-O-C and C=O structures increased with increasing CL/OH ratio.

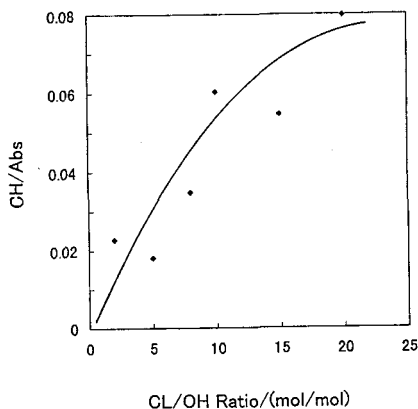


Fig. 9. Relationship between CH absorbance and CL/OH ratio in CAPCL

## Conclusions

- (1)  $T_g$ 's decreased with increasing CL/OH ratio when CL/OH ratio is below 10. This suggests that the PCL chains act as a soft segment in the amorphous region of CAPCL molecules. It was found that the CAPCL's with CL/OH ratios over 15 have a crystalline region in the molecular structure.
- (2)  $T_d$ 's of CAPCL's increased with increasing amounts of PCL chains in CAPCL's. This fact suggests that the thermal degradation of CAPCL with increased chain length seems to occur with more difficulty, since the ratio of thermally unstable saccharide structure in CAPCL decreased comparatively with increasing amounts of PCL.
- (3) The results obtained by TG-FTIR analysis of CAPCL showed that gases with OH, CH, C=O, C-O-C groups were evolved by thermal degradation.



## References

- 1 V.P. Saraf and W.G. Glasser, *J. Appl. Polym. Sci.*, **29**, 1831 (1984)
- 2 V.P. Saraf and W.G. Glasser, *J. Appl. Polym. Sci.*, **30**, 2207 (1985)
3. K. Nakamura, R. Morck, A. Reimann, K.P. Kringstad and H. Hatakeyama, *Polym. Adv. Technol.*, **2**, 41 (1991)
4. K. Nakamura, T. Hatakeyama and H. Hatakeyama, *Polym. Adv. Technol.*, **3**, 151 (1992).
5. H. Yoshida, R. Morck, K.P. Kringstad and H. Hatakeyama, *J. Appl. Polym. Sci.*, **40** 1819 (1990)
6. K. Nakamura, Y. Nishimura, T. Hatakeyama and H. Hatakeyama., *Preparation of Biodegradable Polyurethanes Derived from Coffee Grounds*, in Proceedings for International Workshop on Environmentally Compatible Materials and Recycling Technology in Tsukuba, Japan, November 15-16 (1993), p. 239
7. H. Hatakeyama, S. Hirose, K. Nakamura and T. Hatakeyama, *New types of Polyurethanes Derived from Lignocellulose and Saccharides*, in *Cellulosics: Chemical, Biochemical and Material Aspects*, J. F. Kennedy, G. O. Phillips and P. A. Williams, Eds., Ellis Horwood, 1993, p. 381
8. H. Yoshida, K. Kobashigawa, S. Hirose and H. Hatakeyama, *Molecular Motion of Biodegradable Polyurethanes Derived from Molasses*, in Proceedings for International Workshop on Environmentally Compatible Materials and Recycling Technology in Tsukuba, Japan, November (1993), p. 15
9. N. Morohoshi, S. Hirose, H. Hatakeyama, T. Tokashiki and K. Teruya, *Sen-i Gakkaishi*, **51**, 143 (1995)
10. T. Nakamura, Y. Nishimura, P. Zetterlund, T. Hatakeyama and H. Hatakeyama, *Thermochimica Acta*, **282/283**, 433 (1996)
11. P. Zetterlund, S. Hirose, T. Hatakeyama, H. Hatakeyama and A-C. Albertsson, *Polymer International*, **42**, 1 (1997)
12. M. J. Donnelly, *Polymer International*, **37**, 297 (1995)
13. H. Hatakeyama, K. Kobahigawa, S. Hirose and T. Hatakeyama, *Macromol. Symp.*, **130**, 127 (1998)
14. T. Hatakeyama and F. X. Quinn, *Thermal Analysis*, John Wiley & Sons, Chichester (1994), p.65
15. K. Nakamura, Y. Nishimura, P. Zetterlund, T. Hatakeyama and H. Hatakeyama, *Thermochimica Acta*, **282/283**, 433 (1996)